Journal of the Energy Institute 107 (2023) 101187

Contents lists available at ScienceDirect

Journal of the Energy Institute

journal homepage: www.elsevier.com/locate/joei

CO_2 capture from fluid catalytic crackers via chemical looping combustion: Regeneration of coked catalysts with oxygen carriers

Fatih Güleç [a,b,*], Will Meredith [b], Colin E. Snape [b]

[a] Advanced Materials Research Group, Faculty of Engineering, University of Nottingham, Nottingham, NG7 2RD, UK
[b] Low Carbon Energy and Resources Technologies Research Group, Faculty of Engineering, University of Nottingham, Triumph Road, Nottingham, NG7 2TU, UK

ARTICLE INFO

Handling Editor: Dr. Paul Williams

Keywords:
Chemical looping combustion
Advanced combustion
Fluid catalytic cracking
CO_2 capture
Oxygen carrier

ABSTRACT

Oil refineries are responsible for ~5% of total global CO_2 emissions and approximately 25–35% of these emissions are released from a single unit called Fluid Catalytic Cracking (FCC). Chemical Looping Combustion (CLC) has been recently proposed as a novel CO_2 capture method from the regenerator of FCC units as an integrated process of CLC-FCC. In this study, for the first time, the combustion behaviour of three types of cokes, a model FCC coke (which is a low volatile semi-anthracite coal), and cokes deposited on commercial FCC catalysts by n-hexadecane cracking and Vacuum Gas Oil, were comprehensively investigated with oxygen carriers (Co_3O_4, CuO, and Mn_2O_3) in a fixed-bed reactor at 700–850 °C. The results demonstrate that a high coke combustion efficiency was achieved with CuO (98 vol %), Co_3O_4 (91 vol %), and Mn_2O_3 (91 vol %) at 800 °C for 30 min. CuO was the most effective oxygen carrier, at temperatures greater than 750 °C for 45 min of residence time. These are the regeneration conditions used in the conventional FCC regenerators.

1. Introduction

Heavy industries such as oil refining, cement, and iron-steel, account for ~22% of the global CO_2 emissions [4,30,41,49]. As the largest single source of CO_2 emitter, Fluid Catalytic Cracking (FCC) units are responsible for 20–35% of the total CO_2 emissions [20,49] released from oil refining (which are collectively responsible for ~5% of global CO_2 emissions) [31,48,49]. The CO_2 emissions from the FCC regenerators can be captured by post-combustion capture technologies, such as amine scrubbing [18,42]. Despite post-combustion being a mature technology for CO_2 captures, chemical looping combustion (CLC) and oxy-combustion offer lower energy penalties [15,26,38,54]. In FCC-oxy-combustion, the combustion of coke (regeneration of catalysts) occurs with the oxygen mixed with recycled CO_2 rather than air. However, the process conditions and the effect of CO_2 on coke regeneration in the application of oxy-combustion are needed to be investigated and improved before commercialisation [26,39].

CLC technology is identified as a novel CO_2 capture technology thanks to its inherent separation of CO_2 [35,36,54]. The CLC process is based on oxygen transfer between two interconnected reactors called fuel reactor and air rector, in which oxygen transfer from the air reactor to the fuel reactor via a solid oxygen carrier. In this process, air does not need to mix with fuel for combustion. Firstly, the fuel either solid or gas is introduced to the fuel reactor and oxidised to CO_2 and H_2O by a metal oxide [53] which is reduced to metal or any other reduced form during this reaction. After a condensation and purification step, the pure CO_2 is ready for transport and storage [2]. Subsequently, in the air reactor, the reduced oxygen carrier is oxidised by oxygen in the air stream. The re-oxidised oxygen carrier gets ready for a new combustion cycle. The flue gas from the air reactor contains nitrogen and excess oxygen gases [2,13]. Thanks to the unique CO_2 separation technology, chemical looping can be applicable in a wide range of technologies i.e. combustion, gasification, hydrogen production, direct oxygen production, gas cleaning, coke combustion etc. Since the application of chemical looping technologies have been investigated with various fuels such as fossil fuels i.e. methane, natural gas, syngas, coal, petroleum coke and renewables i.e. biomass, biocoal, biochar, biooil, in various size pilot-scale reactors [26,37,46,53].

Metal oxides play a significant role in the integration of CLC technology [21] to FCC units in which they are used as oxygen suppliers to combust the FCC catalyst cokes in regenerators. CLC technology has been proposed as an energy saving alternative process compare to post- and oxy-combustion capture technologies [33]. This is based on CLC being developed as one of the best alternative processed to amine

---

[*] Corresponding author. Advanced Materials Research Group, Faculty of Engineering, University of Nottingham, Nottingham, NG7 2RD, UK.
E-mail addresses: Fatih.Gulec1@nottingham.ac.uk, Gulec.Fatih@outlook.com (F. Güleç).

https://doi.org/10.1016/j.joei.2023.101187
Received 4 October 2022; Received in revised form 11 January 2023; Accepted 13 January 2023

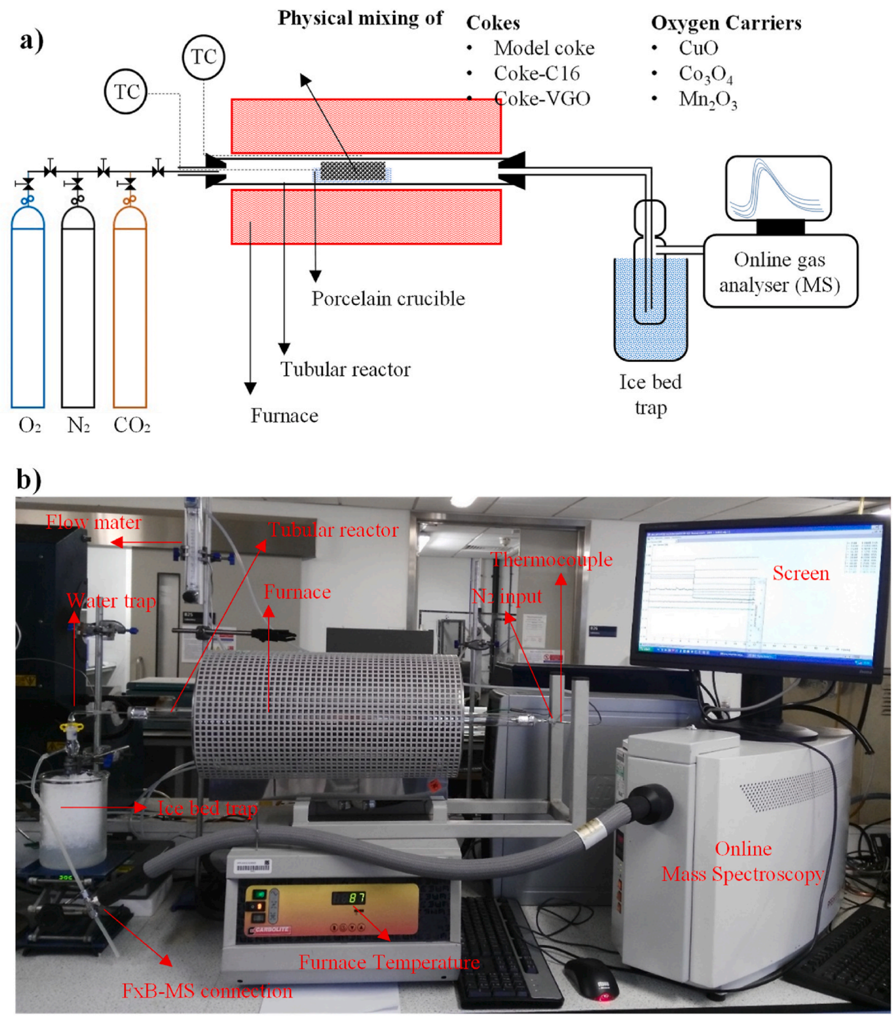

Fig. 1. The experimental set-up of FxB-MS unit, a) Flowchart and b) Picture [27].

scrubbing to minimise the CO_2 capture cost [32] as it does not need a separation process [34,37] unlike post-combustion [18,19,42] or oxy-combustion [14,16,17]. In our previous studies [24–26], CLC integration to FCC was experimentally investigated with a novel CLC-FCC configuration, where the FCC catalysts (equilibrium catalyst – ECat) were modified by reduced form of oxygen carriers (Mn_3O_4, CoO, and Cu_2O) [24,26] using physical mixing [24] and impregnation [27] methods. The reduced oxygen carriers (Mn_3O_4, CoO, and Cu_2O) demonstrated insignificant effects on the yields (coke, gas, and liquid) and selectivity of cracking products [24]. Similar results were also observed for the catalysts prepared by wet-impregnation [27] but the ECat increased coke deposition [27,28]. Complete combustion of a model coke (a semi anthracite coal) was achieved with Mn_2O_3, Co_3O_4, and CuO at 800 °C with stoichiometric ratio of oxygen carrier/coke and 40–60 min of regeneration time [24]. Furthermore, with CuO and Mn_2O_3 modified ECat, higher than 94 vol % of coke combustion was achieved at 750 °C for 45 min [27].

The previously proposed CLC-FCC configuration demonstrated very promising results for the regeneration of FCC catalyst with oxygen carriers [27], where a commercial FCC catalyst was impregnated with oxygen carriers [22,23,40]. Considering the general application of CLC with solid fuels [46,51,53], the direct regeneration of FCC coke with oxygen carriers (without any further modification) can be another possibility. The physical mixing of a model FCC coke with oxygen carriers were previously investigated using a Thermogravimetric Analyser (TGA) [24] and provides very promising combustion efficiency. In this study, for the first time, (i) the combustion behaviour of the FCC cokes was investigated with oxygen carriers (CuO, Co_3O_4 and Mn_2O_3) in a fixed-bed reactor integrated with an online mass spectrometer at a temperature range 700–850 °C and (ii) **t**he impact of mechanical mixing of oxidised oxygen carriers **(**Mn_2O_3**,** Co_3O_4, and CuO**)** on cracking of a model compound (n-hexadecane) was also identified in order to demonstrate the potential impact on cracking products using ASTM D3907-13.

2. Materials and methods

2.1. Preparation of the cokes

Three different cokes were prepared before the CLC tests. The first coke is a model coke (low volatile semi-anthracite coal), showing elemental similarities with FCC coke. The remaining cokes were prepared via cracking of Vacuum Gas Oil (VGO) and model cracking feed (n-hexadecane, $C_{16}H_{34}$). The cracking reactions were investigated over commercial FCC catalyst (supplied by BASF) in a microactivity test (MAT) unit using ASTM D3907-13 [6], the standard method for testing of FCC catalysts. Further information about the MAT unit and test conditions were presented in previous studies [24,27]. The coke deposited on the FCC catalyst were designated "Coke-C16" for the cracking of n-hexadecane and "Coke-VGO" for the cracking of VGO.

Table 1
Proximate and ultimate analyses of the model coke.

Proximate analysis[a] (wt.%)				Ultimate analysis[a] (wt.%)				
TM[b]	VM	FC	Ash	C	H	N	S	O[c]
0.5	16.2	70.3	13.5	86.3	4.3	1.5	2.2	5.7

[a] Dry basis.
[b] as received basis.
[c] Determined by difference. FC: Fixed carbon, TM: Total moisture, VM: Volatile matter.

2.2. Effects of oxidised oxygen carrier on cracking

The catalytic cracking activity of ECat catalysts modified by oxidised oxygen carriers (M-Co_3O_4/ECat, M-CuO/ECat, and M-Mn_2O_3/ECat) were investigated by microactivity test (MAT) [6]. The details of the test conditions and experimental unit were presented in previous studies [24,25,27]. One of the most promising approaches for the use of solid fuels in CLC is the oxygen uncoupling (CLOU) process, where the oxygen carriers release oxygen due to thermal decomposition. As coke combustion with oxygen carriers may occur through a couple of mechanisms. Firstly, the soft coke released from the coke-deposited catalyst can combust with the solid oxygen carriers. Secondly, hard coke can be combusted with the solid phase oxygen carriers via solid-solid interactions between coke and oxygen carriers. The combustion of coke may occur by the gasification of coke thanks to CO_2-Coke and H_2O-Coke interactions. Finally, hard coke combustion may occur with gas-phase oxygen released from the oxygen carriers thanks to their CLOU properties. Considering the hard coke ratio in the FCC catalyst, the CLOU properties is a significantly important and necessary to reach a high level of coke combustion (or catalyst regeneration. This study is therefore focused on CuO, Mn_2O_3, and Co_3O_4 as oxygen carriers thanks to their CLOU properties in which they release oxygen with the decomposition under temperature [2]. The oxygen uncoupling reactions of these metal oxides are previously provided [37,53].

Conversion of n-hexadecane (Equation (1) (overall conversion) and Equation (2) (excluding CLC conversion)), yields (gas, liquid, coke) (Equations (3)–(5)), and selectivities of cracking products such as $C_{5\text{-}15}$ (gasoline), $C_{3\text{-}4}$ (LPG), and $C_{1\text{-}2}$ (dry gas) (Equation (6)) were determined [25,27].

$$Conversion\ (overall, wt.\%) = \frac{w_{C16,0} - w_{C16,f}}{w_{C16,0}} * 100 \tag{1}$$

$$Conversion\ (excluding\ CLC, wt.\%) = \frac{w_{C16,0} - \left(w_{C16,f} + w_{CO_2}\right)}{w_{C16,0}} * 100 \tag{2}$$

$$Gas\ yield\ (wt.\%) = \frac{w_g}{w_{C16,0}} * 100 \tag{3}$$

$$Coke\ yield\ (wt.\%) = \frac{w_C}{w_{C16,0}} * 100 \tag{4}$$

$$Liquid\ yield\ (wt.\%) = \frac{w_{C16,0} - w_{C16,f} - w_g - w_C}{w_{C16,0}} * 100 \tag{5}$$

$$Selectivity\ of\ i\ compounds\ (wt.\%) = \frac{w_i}{\sum w_{products}} * 100 \tag{6}$$

n-hexadecane in feed ($W_{C16,0}$, g), uncracked n-hexadecane in the products ($W_{C16,f}$, g), carbon in carbon dioxide in the products (W_{CO2}, g), coke (W_C, g), total gas products (W_g, g), product i (W_i, g, $C_{1\text{-}2}$, $C_{3\text{-}4}$, $C_{5\text{-}15}$, C_{16+}, and coke), total products ($\Sigma W_{products}$, g, $C_{1\text{-}2}$, $C_{3\text{-}4}$, $C_{5\text{-}15}$, C_{16+}, and Coke).

2.3. Elemental analysis

The elemental analysis of coke (deposited on FCC catalyst) and model coke were investigated by a Leco CHN-628 instrument. Approximately 0.15–0.20 g of used FCC catalyst placed in tin foil cups are dropped from an automated sample carousel to the combustion tube where the combustion temperature held at ~1000 °C [10,29]. The analysis was repeated three times to reduce any systematic error.

2.4. CLC of the cokes in a fixed bed MS (FxB-MS) unit

Combustion of Model coke, Coke-C16 and Coke-VGO with CuO: The combustion of model coke, Coke-C16 and Coke-VGO with CuO was investigated with a fixed-bed MS (FxB-MS) unit (Fig. 1) using the following experimental conditions: 48 mg of Model coke (low volatile semi-anthracite, consisting of 86.3 wt% of carbon and 4.3 wt% of hydrogen) were physically mixed with ~1.3 g of CuO (stoichiometrically required amount of oxygen carriers). Additionally, ~0.9 g of Coke-C16 (consisting of 4.6 wt% of carbon and 0.4 wt% of hydrogen) and ~2.0 g of Coke-VGO (Consisting of 2.1 wt% of carbon and 0.3 wt% of hydrogen) with ~1.4 g of bulk CuO. The prepared mixtures of oxygen carriers and coke were loaded in a horizontal reactor (Fig. 1). The mixture was then heated from ~25 °C to 850 °C with 20 °C/min under inert (N_2) atmosphere (35 ml/min). In CLC tests, the amount of carbon was kept same to get a comparison on the combustion behaviours and products. The combustion gases such as CO_2, H_2, and CH_4 were analysed using an on-line mass spectroscopy (MS).

The combustion percentage for CLC of coke was determined using Equation (7).

$$\text{Combustion (vol. \%)} = \frac{V_{CO_{2,MS}}}{V_{CO_{2,Coke}}} * 100 \tag{7}$$

CO_2 measured by MS in flue gas ($V_{CO2,MS}$, ml), CO_2 determined based on carbon content of coke ($V_{CO2,Coke}$, ml).

Combustion profiles of coke with CuO in TGA and FxB-MS: The combustion of model-coke with CuO was repeated using thermogravimetric analysis (TGA-Discovery) under the same experimental conditions. 48 mg of model coke (consisting of 86.3 wt% of carbon and 4.30 wt% of hydrogen) were physically mixed with ~1.27 g of CuO, which consists of stoichiometrically required amount of oxygen carriers. The mixture of model coke and CuO was loaded in the reactor and heated from ~25 °C to 850 °C with 20 °C/min under an inert (N_2) atmosphere (35 ml/min). Comparison of the combustion profiles in TGA and FxB-MS can also validate the CLC tests investigated by TGA presented in previous study [24]. The TGA tests were triplicated in order to reduce systematic errors.

Effect of oxygen carriers: The coke deposited FCC catalysts were mixed with oxygen carriers, Mn_2O_3, CuO, and Co_3O_4 in order to investigate the effects of oxygen carrier types in order of stoichiometrical amount. For example, ~0.92 g coke deposited FCC catalyst was mixed with ~1.38 g of CuO, ~0.89 g of coke deposited FCC catalyst was mixed with ~2.02 g of Co_3O_4 and ~0.93 g of coke deposited FCC catalyst was mixed with ~4.17 g of Mn_2O_3. Then, the coke combustion was investigated in the FxB-MS unit using the same experimental procedure described above at a combustion temperature of 800 °C. The combustion gases were screened by on-line MS as ion current and transformed to CO_2 flowrate using the calibration graph.

Effect of the CLC temperatures: The effect of temperatures on the combustion was investigated with the mixture of coke deposited FCC catalyst (~0.88 g) and CuO (~1.32 g) in a quartz reactor. The mixture was then heated from 25 °C to the combustion temperatures, 700, 750, 800, and 850 °C, with 20 °C/min as a heating rate under an inert (N_2) atmosphere (35 ml/min).

3. Results and discussion

3.1. Coke characterization

The proximate and ultimate analyses of model coke (a low volatile

Table 2
Element analysis of model coke and FCC cokes prepared in the lab-scale cracking unit (as mentioned in Section 2.1).

Coke type	Coke on catalyst[a]		Coke structure	
	Carbon (C, wt. %) (±0.04)	Hydrogen (H, wt. %) (±0.07)	SC[c] (wt. %)	HC[b] (wt. %)
Model coke	86.3	4.30	18.7	81.3
Coke-C16	4.55	0.37	0.5	99.5
Coke-VGO	2.06	0.31	4.5	96.5

[a] Carbon and hydrogen percentages measured by elemental analysis.

[b] Hard coke, the remaining coke % after solvent extraction for FCC cokes and FC for model coke.

[c] Soft Coke was measured by the differences of 100-HC.

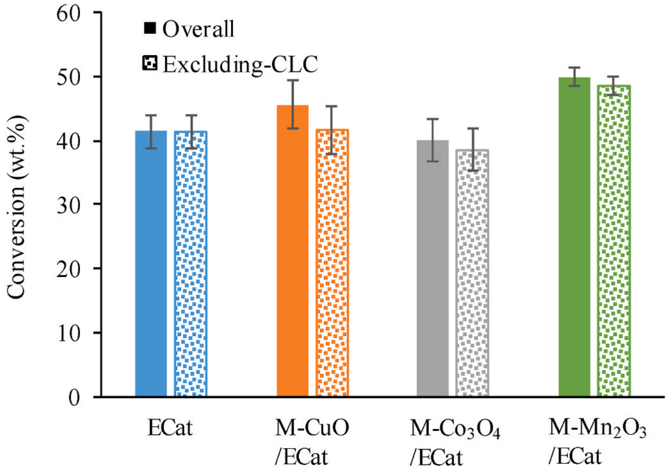

Fig. 2. Conversion of n-hexadecane over the commercial ECat and oxidised oxygen carriers mixed forms (M-CuO/ECat, M-Co_3O_4/ECat, and M-Mn_2O_3/ECat).

semi-anthracite coal) are presented in Table 1. Additionally, the percentage of carbon and hydrogen in coke, and normalised composition are presented in Table 2. The carbon and hydrogen composition in the cokes (model and produced by the cracking of n-hexadecane and VGO) demonstrate similar elemental composition with the FCC coke [9]. However, the soft coke and hard coke distribution in the coke show differences based on the coke type, which may be attributed to the type of cracking feed.

3.2. n-hexadecane cracking over oxidised oxygen carriers mixed with ECat

Fig. 2 demonstrates the conversion of n-hexadecane cracking over M-Mn_2O_3/ECat, M-Co_3O_4/ECat, M-CuO/ECat catalysts. As previously mentioned in Section 2.2, two different conversions were defined; the first one is the overall conversion in which CLC during cracking reaction was included. The second one is excluding CLC conversion, in which the amount of C in the CO_2 produced with additional feedstock combustion with oxidised metal oxide within the cracking reaction was excluded. In terms of the conversion (excluding CLC), the mixing of both CuO and Co_3O_4 with ECat has an insignificant effect on conversion, which was about 40 wt%, whereas the mixing of Mn_2O_3 with ECat slightly enhanced it from 40 wt% to nearly 47 wt% as illustrated in Fig. 2. This increase may be attributed to the volumetrically expansion of catalyst bed after mixing oxygen carriers which increase the residence time of n-hexadecane in the catalyst bed. As the volume of the catalyst bed increased about 25 vol% with the mixing of Mn_2O_3 due to the higher amount of Mn_2O_3 required for the same oxygen capacity compare with Co_3O_4, and CuO (increased only about 3 wt% of bed volume). The mixing of oxidised oxygen carriers increased the overall conversion due to the additional combustion of feedstocks with oxidised oxygen carriers. The differences between overall and excluding CLC conversions are about 4 wt% for M-CuO/ECat and 1 wt% for both M-Co_3O_4/ECat, M-Mn_2O_3/ECat. The differences can be attributed to the reduction stages of oxygen carriers; CuO → Cu, Co_3O_4 → CoO, and Mn_2O_3 → Mn_3O_4+MnO (as demonstrated in XRD patterns Fig. S1) while oxidising (combusting) the FCC feedstocks. This differences also represent the loss of the feedstocks due to the combustion reaction over oxidised oxygen carriers while the cracking reaction occurs. The feedstock loss due to combustion is obviously dependent on oxygen carrier type. The better the low temperature CLC, the greater the loss. The maximum of 4 wt% feedstock lost is not that great and the heat load for cracking will be reduced due to this combustion.

Based on reduction stage calculations and XRD analysis, CuO reduced to Cu with the combustion of liquid hydrocarbons (n-hexadecane) at a low temperature such as 482 °C. The CuO reduction to Cu at such a low temperature has been attributed to the minimal external mass transfer at low combustion temperatures [25]. The reaction between CuO and carbon starts at 482 °C and the reaction between Cu_2O and carbon starts at 624 °C [47]. The product yields and selectivity over M-CuO/ECat, M-Co_3O_4/ECat, and M-Mn_2O_3/ECat are presented in Figs. S2 and S3 in supplementary. The product distribution (analysis with GC) are presented in Figs. S4 and S5 in supplementary. In the presence of CuO, Co_3O_4, and Mn_2O_3 with ECat in the cracking reaction of n-hexadecane have limited impact on the coke yield and product selectivity. The presence of Co_3O_4 and Mn_2O_3 have a similar gas yield, approximately 22 wt%. However, the gas yield was enhanced from about 22 wt% to 33 wt%, which can be attributed to CO_2 production, thanks to the combustion of hydrocarbons with CuO.

3.3. CLC of the cokes in a fixed bed MS (FxB-MS) unit

3.3.1. Combustion profiles of model coke with CuO in FxB-MS and TGA

Fig. 3 demonstrates that the derivative weight (red line) consisted of three weight loss steps, the first one (S-1) had approximately 1.1 wt % at the temperatures between 420 and 600 °C, which must be attributed to removing volatiles from coal and combustion with solid CuO. The low weight loss for the first step may explain the type of model coke, which is a low volatile semi-anthracite coal. These findings are in line with Wang et al. [50], lower volatile matter contents produce lower CO_2 for the first stage in the combustion of LPS and YQ coals with $CuFe_2O_4$. The second one (S-2) had about 1.2 wt % at the temperatures 600–780 °C, which may be due by solid-solid interaction of model coke and CuO. The final one (S-3) was approximately 10.4 wt % at the temperatures 780–850 °C, which must be due to the combustion of FC with oxygen released from CuO. As thermal decomposition of CuO to Cu_2O starts at 790 °C [45] and having a partial pressure of oxygen about $1.0*10^{-3}$ at 800 °C [37].

The reduction of CuO induced by volatile matters released at the temperatures around 400 °C and the combustion of fixed carbon induced by the oxygen supplied by the thermal decomposition of CuO at about 800 °C [45]. The mass loss observed between 450 and 790 °C can be attributed to solid (coke) – solid (CuO) interaction [45]. Similarly, the three TGA reaction steps for the combustion of another coal, Illinois #6, with CuO were also presented by Ref. [46], where the steps were defined at 300–460 °C, 460–550 °C and 550–810 °C.

Furthermore, the investigation of LPS coal combustion with Fe_2O_3 has occurred in three reaction stages, as presented by Ref. [7]. In Fig. 3-b, the weight derivative line (red line) obtained in TGA experiments were compared with the CO_2 evaluation (green line) obtained from the FxB-MS unit. The CO_2 recorded by MS demonstrates three different steps, which are in line with the steps measured by the TGA experiments. However, the derivative weight continued to decrease after 60 min, although no CO_2 is released after that point. This further

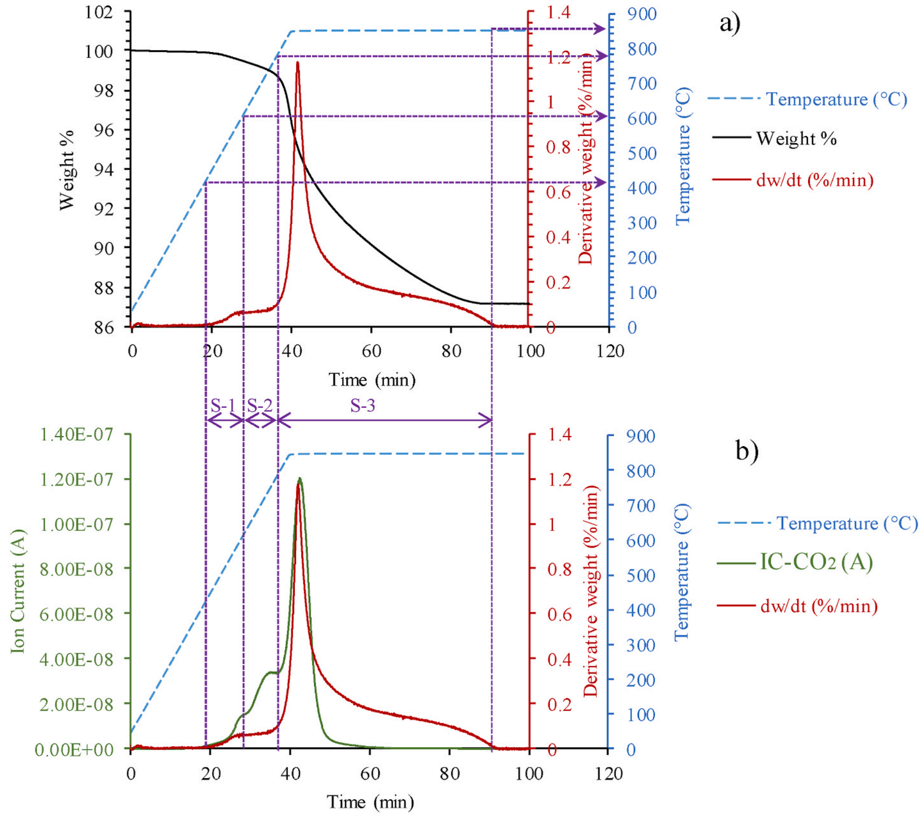

Fig. 3. TGA and FxB-MS profiles of combustion (model coke with CuO at 850 °C), **a)** TGA results, **b)** comparison of TGA and FxB-MS results ("IC" refers to ion current measured by MS).

decrease may be attributed to excessive oxygen released from excess oxygen carriers since some of the volatiles was removed from the mixture without combustion or adding a slightly higher oxygen carrier than required.

3.3.2. *Identification of the CLC products (flue gas)*

Fig. 4 shows that the MS detected three main gases; H_2 and CH_4, and a large amount of CO_2, released from combustion of both model coke (Fig. 4-a) and Coke-C16 (Fig. 4-b) with CuO. Additionally, the intensity of the CO_2 peaks was about the same since an equal amount of carbon was combusted in both experiments.

As mentioned previously, the model coke combustion profile with CuO presents in three steps at (i) 420–600 °C, (ii) 600–780 °C, and (iii) 780–850 °C (Figs. 3 and 4-a), whilst the combustion of Coke-C16 with CuO occurred in one stage, which started from ~580 °C and accelerated after ~700 °C. The amount of coke deposited on commercial FCC catalyst was 4.8 wt % after the cracking of n-hexadecane, which was composed of 0.5 wt % soft coke and 99.5 wt % of hard coke (Table 2). The combustion step for soft coke was not, therefore, visible due to the low amount of soft coke. Furthermore, low-temperature combustion, (starting at ~580 °C and accelerating at ~700 °C) may be attributed to the solid-solid interaction thanks to the coke dispersion on the catalyst surface. Although, below 713 °C, the decomposition of CuO is not thermodynamically favourable, oxidation of carbon with CuO can be favourable between 200 and 1000 °C based on the positive Gibbs free energy analysis [47]. The carbon in the coke may induce Cu–O bond-breaking process to initiate the combustion at a temperature of 580 °C. Similarly, the combustion of pure carbon with CuO occurred at 480 °C [47]. Additionally, the shift on the CO_2 to the lower temperature for Coke-C16 combustion with CuO may also be attributed to the coke dispersion over the catalyst unlike bulk model coke. The combustion of model coke might have driven by the shrinking core model where the outer carbon combusts first and then the combustion continuous to inside [12]. Thus, a clear transition step due to the solid-solid interaction was observed for model coke combustion with CuO in Fig. 4. In terms of Coke-C16, the transition stage, however, connected with the hard coke combustion with oxygen released from thermal decomposition of oxygen carriers thanks to the coke dispersion on the catalyst surface, which may enable high interaction surface of coke and CuO.

3.3.3. *Combustion of model coke, Coke-C16, and Coke-VGO with CuO*

It is important to compare the combustion behaviours of the cokes; (i) produced by the vacuum gas oil (Coke-VGO) cracking, which is a real feedstock, (ii) produced by cracking of model compound (Coke-C16), n-hexadecane, and (iii) model coke, with CuO, as shown in Fig. 5. The Coke-VGO and model coke combustions started at a temperature of ~420 °C, which is most probably due to the soft coke combustion in the Coke-VGO or volatiles combustion in model coke with solid CuO. Furthermore, an apparent delay in the combustion of hard coke for Coke-VGO can be observed compared with that of Coke-C16, which may be attributed to various coke composition. As the properties of coke such as location, nature and amount depend on the cracking feed composition, catalyst type and reaction conditions [8]. Cerqueira et al. [11] categorised the cokes in five main groups; catalytic coke, catalyst to oil coke, thermal coke, additive coke, and contaminant coke. Additionally, as demonstrated previously, the Coke-C16 contained a minimal amount of soft coke. However, complete combustion was achieved for the Coke-C16 and Coke-VGO using stoichiometrically required amount of CuO as an oxygen supplier, as indicated in Table 3. Furthermore, high combustion (96 vol %) was also achieved for model coke combustion with CuO at same conditions.

3.3.4. *Effect of CLC temperature*

Although high temperatures (higher than 800 °C) are usually investigated for the CLC application with solid fuels [1,51,52], it is preferable to 650–760 °C for the coke combustion due to the limitations

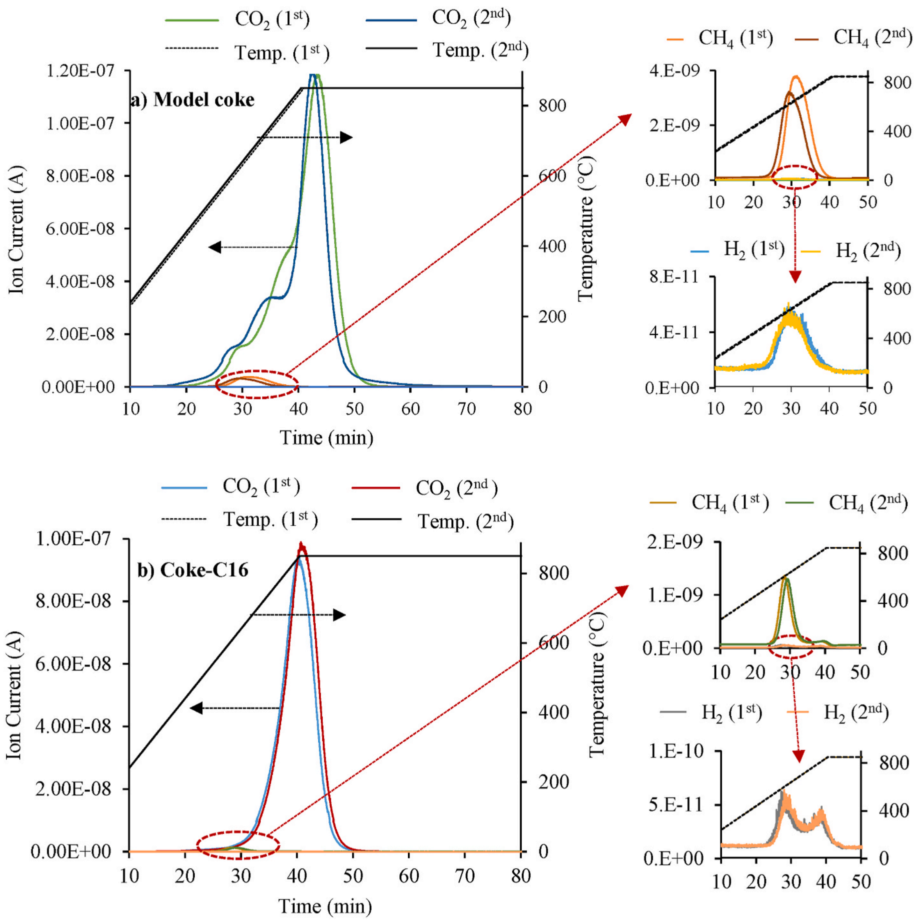

Fig. 4. Comparison of the combustion products of a) model coke, which is a semi-anthracite, and b) Coke-C16 (deposited on commercial catalyst during n-hexadecane cracking at 482 °C), with stoichiometrically required amount CuO in FxB-MS unit at 850 °C (1st and 2nd refer replicate tests).

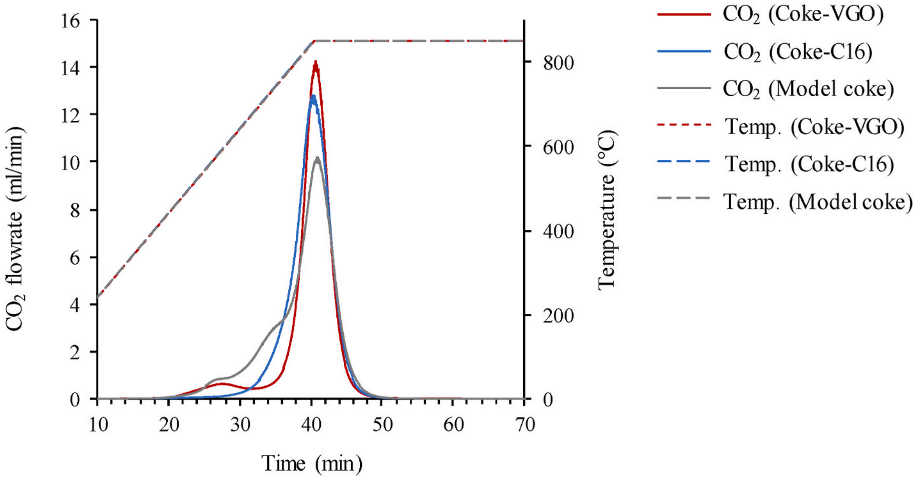

Fig. 5. Comparison of the combustion behaviour of Coke-C16, Coke-VGO and model coke with CuO in FxB-MS unit at 850 °C.

of commercial catalyst regeneration [11,43]. Fig. 6 and Table 4 show the CO_2 flowrates produced by the Coke-C16 combustion with CuO at four different temperatures and combustion %, respectively. Fig. 6 and Table 4 demonstrate a decrease in the combustion efficiency with decreasing the combustion temperature. Whereas the efficiency of coke combustion with CuO is above 90 vol % at the temperatures higher than 750 °C, this was reduced to 59 vol % at 700 °C. The required time to reach complete combustion at 700 °C is much higher than that at the temperatures higher than 750 °C. This decrease in the combustion may be attributed to the oxygen releasing rate of CuO being slower at lower temperatures [3,37,44]. The lower temperatures result in lower partial pressure of oxygen from CuO, which can be observed as a long tail in Fig. 6. However, as clearly seen from Table 4, >90 vol % of coke was removed with CuO at temperatures higher than 750 °C for 45 min which is within the range of standard regenerator operating conditions [5,11,43].

Table 3

Combustion of Coke-C16, Coke-VGO and model coke with CuO in FxB-MS unit at 850 °C.

Coke source	Oxygen carrier	Temperature (°C)	$V_{CO2,\ Coke}$[a] (ml)	$V_{CO2,\ MS}$[b] (ml)	Combustion (vol. %)
Model coke	CuO	850	80.5	77.5	96
Coke-C16	CuO	850	78.6	78.2	99
Coke-VGO	CuO	850	71.9	71.1	99

[a] Maximum CO_2 volume can be produced.

[b] Measured CO_2 volume in Fig. 5.

3.3.5. Effect of oxygen carrier

The effect of CuO, Co_3O_4, and Mn_2O_3 on the Coke-C16 combustion were investigated under the same experimental conditions and the results presented in Fig. 7 and Table 5. There was no, or minimal CO_2 observed due to the soft coke combustion with Co_3O_4 and CuO, was shown in Fig. 7. The hard coke combustion with Mn_2O_3 was shifted to a lower temperature and completed earlier compared to the combustion with both CuO and Co_3O_4. The differences in the combustion times and shifting on the CO_2 may be attributed to the oxygen releasing temperature and capacity of these oxygen carriers at the same conditions [2,3,44]. 90 vol% of coke was combusted with CuO, Co_3O_4, and Mn_2O_3 for less than 30 min at a temperature of 800 °C, as shown in Table 5. The results are in line with model coke combustion with bulk oxygen carriers in a TGA presented in the previous paper [24], in which the combustion efficiency of model coke was 90 wt% for Mn_2O_3 (12 min) and Co_3O_4 (15 min), and 100 wt% for CuO (19 min).

4. Conclusions

The cracking reactions, the conversion, yield (liquid, gas, solid), and selectivity did not show a significant change in the presence of CuO, Co_3O_4, and Mn_2O_3. However, these oxygen carriers result in limited combustion (<4 wt% of feedstocks) due to the CuO reduction to Cu, and <1 wt% due to the reduction of Mn_2O_3 to Mn_3O_4, and Co_3O_4 to CoO during the cracking reaction. The feedstock loss due to combustion is obviously dependent on oxygen carrier type and reduction stages of these oxygen carriers. Considering the oxygen carriers quantity used in this experiment (stoichiometric amount) for the regeneration of coke, circulation of these oxygen carriers to the FCC riser reactor does not have a significant impact on cracking. The maximum of 4 wt% feedstock lost is not that great and the heat load for cracking will be reduced due to this combustion. The model coke, Coke-C16, and Coke-VGO had similar element compositions but with a different level of soft and hard cokes. The CLC of model coke with CuO took place in three distinct steps at 420–600 °C, 600–780 °C, and 780–850 °C, depending on the amount of soft coke. However, the combustion of Coke-C16 with CuO occurred in a single stage starting at ~580 °C and accelerated at ~700 °C. Complete combustion (99 vol %) was achieved for the CLC of Coke-C16 and Coke-VGO with the stoichiometrically required amount of CuO at 850 °C. Furthermore, a high combustion (96 vol %) was also achieved for the coke combustion at 850 °C with CuO. As for oxygen carriers, high combustion of Coke-C16 was achieved with CuO (98 vol %) and followed by Co_3O_4 (91 vol %), and Mn_2O_3 (91 vol %) at 800 °C for 30 min. For, Coke-C16 with CuO, >93 vol % was achieved at the temperature of >750 °C for the residence time of 45 min.

Authorship contribution

Fatih Güleç: Conceptualization, Formal analysis, Methodology, Investigation, Funding acquisition, Validation, Visualization, Project administration, Writing - original draft, Writing - review & editing. **Will Meredith:** Conceptualization, Funding acquisition, Supervision, Writing - review & editing. **Colin E. Snape:** Conceptualization, Methodology, Supervision, Project administration, Funding acquisition, Writing - review & editing.

Declaration of competing interest

The authors declare that they have no known competing financial

Table 4

Combustion efficiency at temperature ranges 700–850 °C.

Coke source	Oxygen carrier	Temperature (°C)	$V_{CO2,\ Coke}$[a] (ml)	$V_{CO2,\ MS}$[b] (ml)	Combustion (vol. %)
Coke-C16	CuO	850	78.6	78.2	99
Coke-C16	CuO	800	78.6	77.4	98
Coke-C16	CuO	750	74.8	69.5	93
Coke-C16	CuO	700	74.8	44.3	59

[a] Maximum CO_2 volume can be produced.

[b] Measured CO_2 volume in Fig. 6.

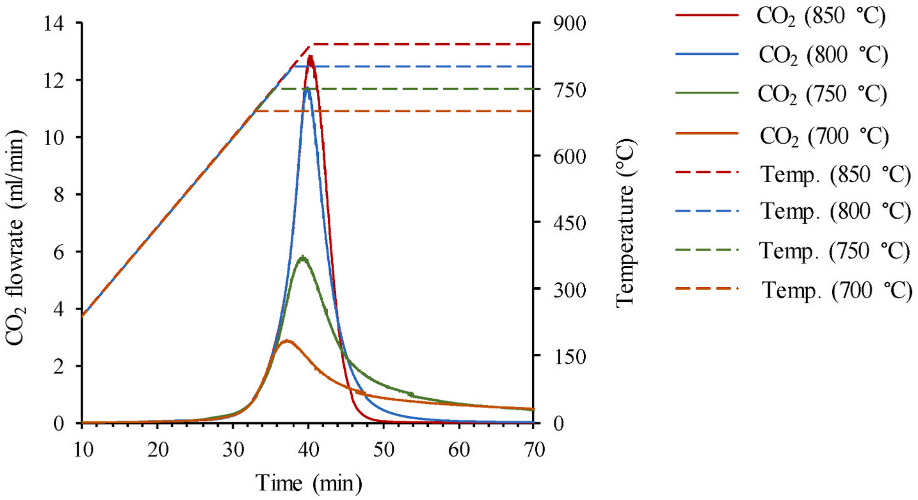

Fig. 6. Effects of temperatures (700–850 °C) on Coke-C16 combustion with CuO in FxB-MS.

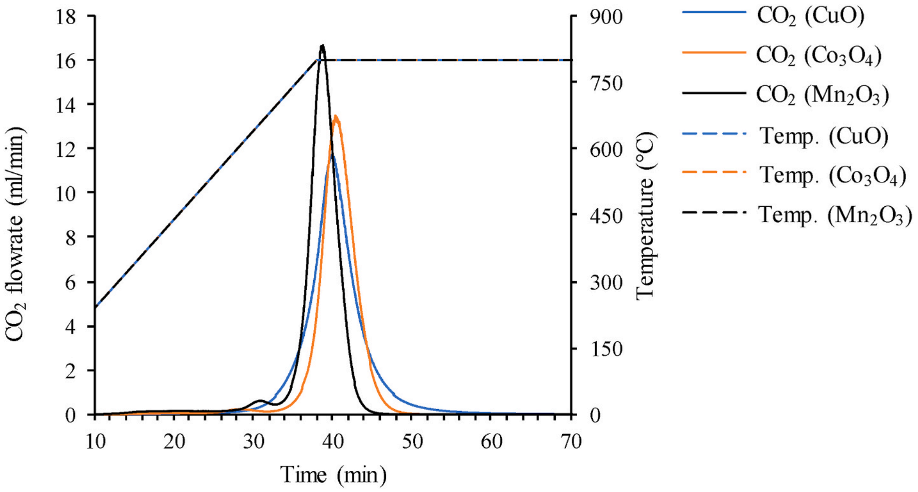

Fig. 7. Effects of CuO, Co_3O_4, and Mn_2O_3 on the Coke-C16 combustion in FxB-MS unit at 800 °C.

Table 5
Combustion efficiency of Coke-C16 with CuO, Co_3O_4, and Mn_2O_3.

Coke source	Oxygen carrier	Temperature (°C)	$V_{CO2, Coke}$[a] (ml)	$V_{CO2, MS}$[b] (ml)	Combustion (vol. %)
Coke-C16	CuO	800	78.6	77.4	98
Coke-C16	Co_3O_4	800	75.6	68.7	91
Coke-C16	Mn_2O_3	800	79.6	72.7	91

[a] Maximum CO_2 volume can be produced.
[b] Measured CO_2 volume in Fig. 7.

interests or personal relationships that could have appeared to influence the work reported in this paper.

Acknowledgements

This research was partially funded and supported by University of Nottingham under “FPVC Research Acceleration Fund” and “Advanced Materials Research Group (AMRG) Early Carrier Researcher Collaboration Fund”.

Appendix A. Supplementary data

Supplementary data to this article can be found online at https://doi.org/10.1016/j.joei.2023.101187.

References

[1] M. Abián, A. Abad, M.T. Izquierdo, P. Gayán, F. Luis, F. García-Labiano, J. Adánez, Titanium substituted manganese-ferrite as an oxygen carrier with permanent magnetic properties for chemical looping combustion of solid fuels, Fuel 195 (2017) 38–48.

[2] J. Adanez, A. Abad, F. Garcia-Labiano, P. Gayan, F. Luis, Progress in chemical-looping combustion and reforming technologies, Prog. Energy Combust. Sci. 38 (2) (2012) 215–282.

[3] I. Adánez-Rubio, P. Gayán, A. Abad, F. García-Labiano, L. de Diego, J. Adánez, Kinetic analysis of a Cu-based oxygen carrier: relevance of temperature and oxygen partial pressure on reduction and oxidation reactions rates in chemical looping with oxygen uncoupling (CLOU), Chem. Eng. J. 256 (2014) 69–84.

[4] M. Ali, R. Saidur, M. Hossain, A review on emission analysis in cement industries, Renew. Sustain. Energy Rev. 15 (5) (2011) 2252–2261.

[5] A. Arbel, Z. Huang, I.H. Rinard, R. Shinnar, A.V. Sapre, Dynamic and control of fluidized catalytic crackers. 1. Modeling of the current generation of FCC's, Ind. Eng. Chem. Res. 34 (4) (1995) 1228–1243.

[6] ASTM, Standard Test Method for Testing Fluid Catalytic Cracking (FCC) Catalysts by Microactivity Test, D3907-13, ASTM International, 2013.

[7] W. Baowen, W. Wei-shu, G. Chuan-chang, Z. Hai-bo, Z. Ying, Z. Chu-guang, TGA-FTIR Investigation of the Chemical Looping Combustion by Coal with a CuO-Fe 2 O 3 Combined Oxygen Carrier, Electric Information and Control Engineering (ICEICE), 2011 International Conference on, IEEE, 2011, pp. 2724–2727.

[8] O. Bayraktar, E. Kugler, Coke content of spent commercial fluid catalytic cracking (FCC) catalysts, J. Therm. Anal. Calorim. 71 (3) (2003) 867–874.

[9] B. Behera, P. Gupta, S.S. Ray, Structure and composition of hard coke deposited on industrial fluid catalytic cracking catalysts by solid state 13 C nuclear magnetic resonance, Appl. Catal. Gen. 466 (2013) 123–130.

[10] M. Bird, C. Keitel, W. Meredith, 4 Analysis of biochars for C, H, N, O and S by elemental analyser, in: Biochar: A Guide to Analytical Methods, 39, 2017.

[11] H. Cerqueira, G. Caeiro, L. Costa, F.R. Ribeiro, Deactivation of FCC catalysts, J. Mol. Catal. Chem. 292 (1–2) (2008) 1–13.

[12] F. Chejne, J. Hernandez, W. Florez, A. Hill, Modelling and simulation of time-dependent coal combustion processes in stacks, Fuel 79 (8) (2000) 987–997.

[13] P. Cho, T. Mattisson, A. Lyngfelt, Comparison of iron-, nickel-, copper-and manganese-based oxygen carriers for chemical-looping combustion, Fuel 83 (9) (2004) 1215–1225.

[14] L.F. de Mello, G.T. Moure, O.R. Pravia, L. Gearhart, P.B. Milios, Oxy-combustion for CO2 capture from fluid catalytic crackers (FCC), in: E. Lars (Ed.), Carbon Dioxide Capture for Storage in Deep Geologic Formation-Results from the CO2 Capture Project, CPL Press, 2009, pp. 31–42.

[15] L.F. de Mello, R.D. Pimenta, G.T. Moure, O.R. Pravia, L. Gearhart, P.B. Milios, T. Melien, A technical and economical evaluation of CO2 capture from FCC units, Energy Proc. 1 (1) (2009) 117–124.

[16] L.F. de Mello, R. Gobbo, G.T. Moure, I. Miracca, Oxy-combustion technology development for fluid catalytic crackers (FCC)–large pilot scale demonstration, Energy Proc. 37 (2013) 7815–7824.

[17] L.F. de Mello, R. Gobbo, G.T. Moure, I. Miracca, FCC oxy-fuel demonstration at petrobras shale industrial business unit, in: K.F. Gerdes (Ed.), Carbon Dioxide Capture for Storage in Deep Geologic Formations-Results from the CO2 Capture Project, CPL Press, 2015, pp. 51–65.

[18] R. Digne, F. Feugnet, A. Gomez, A technical and economical evaluation of CO2 capture from fluidized catalytic cracking (FCC) flue gas, Oil. Gas Sci. Technol. –Revue d'IFP Energies nouvelles 69 (6) (2014) 1081–1089.

[19] A. Elkamel, M. Ba-Shammakh, P. Douglas, E. Croiset, An optimization approach for integrating planning and CO2 emission reduction in the petroleum refining industry, Ind. Eng. Chem. Res. 47 (3) (2008) 760–776.

[20] EPA, Available and Emerging Technologies for Reducing GHG Emissions from Petroleum Refining, U.S. Environmental Protection Agency, 2010.

[21] X. Feng, Z. Li, S. Lin, S. Tian, K. Li, Enhanced performance of red mud for chemical-looping combustion of coal by the modification of transition metal oxides, J. Energy Inst. 102 (2022) 22–31.

[22] F. Güleç, A. Niftaliyeva, A. Karaduman, Selective synthesis of 2, 6-triad dimethylnaphthalene isomers by disproportionation of 2-methylnaphthalene over mesoporous MCM-41, Res. Chem. Intermed. 44 (12) (2018) 7205–7218.

[23] F. Güleç, A. Özen, A. Niftaliyeva, A. Aydın, E.H. Şimşek, A. Karaduman, A kinetic study on methylation of naphthalene over Fe/ZSM-5 zeolite catalysts, Res. Chem. Intermed. 44 (1) (2018) 55–67.

[24] F. Güleç, W. Meredith, C.-G. Sun, C.E. Snape, A novel approach to CO2 capture in fluid catalytic cracking—chemical looping combustion, Fuel 244 (2019) 140–150.

[25] F. Güleç, W. Meredith, C.-G. Sun, C.E. Snape, Selective low temperature chemical looping combustion of higher alkanes with Cu-and Mn-oxides, Energy 173 (2019) 658–666.

[26] F. Güleç, W. Meredith, C.E. Snape, Progress in the CO2 capture technologies for fluid catalytic cracking (FCC) units—a review, Front. Energy Res. 8 (2020).

[27] F. Güleç, W. Meredith, C.-G. Sun, C.E. Snape, Demonstrating the applicability of chemical looping combustion for the regeneration of fluid catalytic cracking catalysts, Chem. Eng. J. 389 (2020), 124492.

[28] F. Güleç, A. Erdogan, P.T. Clough, E. Lester, Investigation of the hydrodynamics in the regenerator of fluid catalytic cracking unit integrated by chemical looping combustion, Fuel Process. Technol. 223 (2021), 106998.

[29] F. Güleç, L.M.G. Riesco, O. Williams, E.T. Kostas, A. Samson, E. Lester, Hydrothermal conversion of different lignocellulosic biomass feedstocks–Effect of the process conditions on hydrochar structures, Fuel 302 (2021), 121166.

[30] IEA, CO2 Emissions from Fuel Combustion, 2016.

[31] G. John, B. John, C. Zhenlin, G. Amit, G. Dario, R. Hans Holger, S. Dale, W. Robert, Sources of CO2, in: B. Metz, O. Davidson, H. De Coninck, M. Loos, L. Meyer (Eds.), IPCC Special Report on Carbon Dioxide Capture and Storage. Intergovernmental Panel on Climate Change, Working Group III, 2005, pp. 75–104.

[32] H.R. Kerr, Capture and separation technology gaps and priority research needs, in: D.C. Thomas, S.M. Benson (Eds.), Carbon Dioxide Capture for Storage in Deep Geologic Formationse Results from the CO2 Capture Project, Elsevier, Oxford, UK, 2005.

[33] H.R. Kerr, Capture and separation technology gaps and priority research needs-, in: S.M. Benson (Ed.), Carbon Dioxide Capture for Storage in Deep Geological Formations-Results from the CO2 Capture Project, Elsevier, Oxford, UK, 2005.

[34] E. Ksepko, R.V. Siriwardane, H. Tian, T. Simonyi, M. Sciazko, Effect of H2S on chemical looping combustion of coal-derived synthesis gas over Fe–Mn oxides supported on sepiolite, ZrO2, and Al2O3, Energy Fuel. 26 (4) (2012) 2461–2472.

[35] Y. Li, J. Liu, F. Liu, Y. Yang, Influence of doping Al on the reactivity performance of Cu–Fe spinel-type oxygen carrier during chemical-looping combustion, J. Energy Inst. 105 (2022) 25–32.

[36] Y. Long, Z. Gu, S. Lin, K. Yang, X. Zhu, Y. Wei, H. Wang, K. Li, NiO and CuO coated monolithic oxygen carriers for chemical looping combustion of methane, J. Energy Inst. 94 (2021) 199–209.

[37] T. Mattisson, A. Lyngfelt, H. Leion, Chemical-looping with oxygen uncoupling for combustion of solid fuels, Int. J. Greenh. Gas Control 3 (1) (2009) 11–19.

[38] T. Melien, S.B. Roijen, Economics, in: Carbon Dioxide Capture for Storage in Deep Geologic Formations, 3, 2009, pp. 237–264.

[39] I. Miracca, D. Butler, CO2 capture from A fluid catalytic cracking unit: technical/economical evaluation, in: Carbon Dioxide Capture for Storage in Deep Geologic Formations–Results from the CO2 Capture Project, 4, 2015, pp. 67–81.

[40] A. Niftaliyeva, F. Güleç, A. Karaduman, Methylation of 2-methylnaphthalene over Metal-Impregnated Mesoporous MCM-41 for the Synthesis of 2, 6-triad Dimethylnaphthalene Isomers, Research on Chemical Intermediates, 2020, pp. 1–14.

[41] NRC, Advancing the Science of Climate Chance, National Research Council, The National Academies Press, Washington, DC, USA, 2010.

[42] P. Peng, Y. Zhuang, The evaluation and comparison of carbon dioxide capture technologies applied to FCC flue gas, in: Advanced Materials Research, Trans Tech Publ, 2012, pp. 1479–1482.

[43] D.J. Rawlence, K. Gosling, FCC catalyst performance evaluation, Appl. Catal. 43 (2) (1988) 213–237.

[44] M. Rydén, H. Leion, T. Mattisson, A. Lyngfelt, Combined oxides as oxygen-carrier material for chemical-looping with oxygen uncoupling, Appl. Energy 113 (2014) 1924–1932.

[45] A. Shabani, M. Rahman, D. Pudasainee, A. Samanta, P. Sarkar, R. Gupta, Evaluation of ash-free coal for chemical looping combustion-part I: thermogravimetric single cycle study and the reaction mechanism, Can. J. Chem. Eng. 95 (4) (2017) 623–633.

[46] R. Siriwardane, H. Tian, G. Richards, T. Simonyi, J. Poston, Chemical-looping combustion of coal with metal oxide oxygen carriers, Energy Fuel. 23 (8) (2009) 3885–3892.

[47] R. Siriwardane, H. Tian, D. Miller, G. Richards, T. Simonyi, J. Poston, Evaluation of reaction mechanism of coal–metal oxide interactions in chemical-looping combustion, Combust. Flame 157 (11) (2010) 2198–2208.

[48] J. van Straelen, F. Geuzebroek, N. Goodchild, G. Protopapas, L. Mahony, CO2 capture for refineries, a practical approach, Energy Proc. 1 (1) (2009) 179–185.

[49] J. van Straelen, F. Geuzebroek, N. Goodchild, G. Protopapas, L. Mahony, CO2 capture for refineries, a practical approach, Int. J. Greenh. Gas Control 4 (2) (2010) 316–320.

[50] B. Wang, R. Yan, H. Zhao, Y. Zheng, Z. Liu, C. Zheng, Investigation of chemical looping combustion of coal with CuFe2O4 oxygen carrier, Energy Fuel. 25 (7) (2011) 3344–3354.

[51] L. Wang, W. Qin, L.N. Wu, X.Q. Hu, M.Z. Gao, J.J. Zhang, C.Q. Dong, Y.P. Yang, Experimental study on coal chemical looping combustion using CuFe2O4 as oxygen carrier, in: Advanced Materials Research, Trans Tech Publ, 2013, pp. 1387–1390.

[52] B. Wang, C. Gao, W. Wang, F. Kong, C. Zheng, TGA-FTIR investigation of chemical looping combustion by coal with CoFe2O4 combined oxygen carrier, J. Anal. Appl. Pyrol. 105 (2014) 369–378.

[53] P. Wang, N. Means, D. Shekhawat, D. Berry, M. Massoudi, Chemical-looping combustion and gasification of coals and oxygen carrier development: a brief review, Energies 8 (10) (2015) 10605–10635.

[54] B. Wang, C. Guo, B. Xu, X. Li, J. Ma, D. Mei, Z. Zhou, Effects of pressure on the chemical looping combustion of coal with CuFe2O4 combined oxygen carrier, J. Energy Inst. 100 (2022) 22–32.